Journal of the Taiwan Institute of Chemical Engineers 61 (2016) 261–269

Contents lists available at ScienceDirect

Journal of the Taiwan Institute of Chemical Engineers

journal homepage: www.elsevier.com/locate/jtice

Study of physical–chemical properties and catalytic activities of $ZnCr_2O_4$ spinel nano oxides obtained from different methods—Modeling the synthesis process by response surface methodology and optimization by genetic algorithm

S.A. Hosseini [a,*], M.C. Alvarez-Galvan [b]

[a] Department of Applied Chemistry, Faculty of Chemistry, Urmia University, 57159, Urmia, Iran
[b] Instituto de Catálisis y Petroleoquímica, CSIC, Cantoblanco, E-28049 Madrid, Spain

ARTICLE INFO

Article history:
Received 30 June 2015
Revised 5 November 2015
Accepted 28 December 2015
Available online 18 January 2016

Keywords:
Zinc chromite
Supported catalyst
Nano-oxide
Response surface design

ABSTRACT

Physicochemical properties of zinc chromite spinel obtained by sol–gel combustion, co-precipitation, and pechini methods were characterized by XRD, FTIR, SEM and TPR and studied as catalysts for the catalytic combustion of toluene. The sample obtained by pechini method showed the highest activity in the catalytic combustion of toluene. Supported zinc chromite samples based on ZSM-5 and γ-Al_2O_3 were prepared by the pechini method with the ratio of spinel to support 2:1. Supported catalysts increased the rate of toluene conversion which is ascribed to a higher surface area and greater reducibility of zinc chromite in the supported catalysts. These factors also explain the better catalytic performance of $ZnCr_2O_4$/ZSM-5 compared than $ZnCr_2O_4$–Al_2O_3. The effects of synthesis factors on activity of catalysts were studied by response surface methodology. The model predicted that the relative importance of factors is as follows: calcination temperature > [citrate/nitrate ratio] > [citrate/EG ratio]. The optimization condition was predicted by genetic algorithm where the optimum conditions were resulted at levels −1, −1, and 0 of calcination temperature, [citrate/nitrate], and [citrate/EG], respectively.

1. Introduction

The removal of volatile organic compounds (VOCs) remains nowadays a challenge for chemists, engineers, and technologists. VOCs are considered as air pollutants, because of both direct (toxic or malodorous nature) and indirect (ozone precursors) harmful effects to human health [1]. In particular, toluene, and aromatic volatile organic compounds, are present in various gas exhaust streams and can cause severe environmental hazards [2]. Catalytic oxidation has been identified as one of the most promising ways to reduce VOC emissions because the reaction temperature is much lower than that required for thermal incineration. The advantage of low oxidation temperature is the reduction of the fuel consumption, particularly for the treatment of large volumes of air containing VOC in low concentrations [3]. In addition, catalytic combustion targets destruction of the pollutant compounds rather than transferring the pollutant to another phase, as is the case for condensation and adsorption technologies [4].

The catalysts used for the abatement of VOCs emissions are mainly divided into two categories: noble metals and transition metal oxides. Transition metal oxides are generally less active than noble metal catalysts, but are much cheaper and may be considered as a suitable alternative [5]. In spite of individual oxides, mixed oxides present improved properties, especially as the environmental catalysts.

Spinel-type mixed oxides are represented by the chemical formula AB_2O_4 where A ions are generally divalent cations occupying tetrahedral sites and B ions are trivalent cations in octahedral sites [6]. Spinel and spinel-like are attractive subjects for continuous scientific interest and have been deeply investigated in materials sciences, because of their physico-chemical properties. Due to their remarkable catalytic properties including high melting points, the metal oxide composites with spinel structure are increasingly being investigated as catalysts for the treatment of environmental pollutants, such as ozone decomposition [7], nitrogen oxides decomposition [8], sulfur oxide removal [9], and others [10]. Later, Kim et al. reported that the spinel type cobalt chromite ($CoCr_2O_4$) catalyst showed good activities for the decomposition of trichloroethylene [11]. Zavyalova et al. have used AB_2O_4 (where A = Co, Cu and B = Cr, Co) as catalysts for the catalytic combustion of hexane [12].

* Corresponding author. Tel.: +98 4432752026; fax: +98 4432755294.
E-mail address: s_ali_hosseini@yahoo.com (S.A. Hosseini).

http://dx.doi.org/10.1016/j.jtice.2015.12.024
1876-1070/

Specific surface area of spinels is relatively low and it is clear that the synthesis method plays a crucial role in order to increase this parameter, which it is crucial to have a good catalytic performance of the mixed oxides [13,14].

Recently we studied the performance of MCr_2O_4 (M = Cu, Co, Zn, Mn, Ni), MMn_2O_4 (M = Cu, Co, Ni, Zn) and CuX_2O_4 (X = Cr, Mn, Co) spinels synthesized by sol gel combustion method for the combustion of 2-propanol [2,15,16,17]. Sol gel combustion gives only moderate improvements in the specific surface area, and it is almost essential to support these spinel materials for high space velocity applications. Among all studied catalysts, $ZnCr_2O_4$ showed the highest activity and also exhibited photocatalytic activity [18].

The primary goal of this work was the optimization of synthesis conditions of spinel oxide catalysts with desired crystal structure and high specific surface area. For this purpose we selected $ZnCr_2O_4$ as a model of spinel mixed oxide and applied three conventional methods for synthesis of nanocatalysts, *i.e.* sol gel combustion, co-precipitation, and pechini methods. The samples obtained by these methods were named as $ZnCr_2O_4$ (SGC), $ZnCr_2O_4$ (CP), and $ZnCr_2O_4$ (Pech), respectively. The catalytic performance of these catalysts was evaluated in the catalytic combustion of toluene and the relationships between physical–chemical properties and catalytic activity was correlated. Then, the influence of supporting $ZnCr_2O_4$ over two high surface area supports, *i.e.* ZSM-5 and γ-Al_2O_3 on the catalytic activity of zinc chromite spinel was studied. Finally, in order to obtain an insight about the importance of synthesis factors and to optimize the suitable method, optimization modeling by response surface methodology (RSM) has been performed. The characterization of catalysts was carried out by XRD, in-situ XRD, FTIR, SEM and TPR techniques.

On the other hand, the effects of synthesis factors, such as calcination temperature, citric acid amount and [citrate/EG] ratio on catalytic activity, were studied by response surface methodology (RSM). Response surface methodology (RSM) is a combination of mathematical and statistical techniques and is useful to analyze the effects of independent factors on the response of the system. In this method the predetermination of objective function and the factors is not needed [19]. This technique has already been used in optimization of catalytic process.

The genetic algorithm (GA) methodology was applied to find the optimum conditions of catalyst that maximize toluene conversion. The genetic algorithm is a stochastic search technique based on the mechanism of natural selection and natural genetics. It is applied to solve the optimization problems that are not well suited for standard optimization algorithms. The GA starts with an initial random population, which presents the first generation. The population consists of some chromosomes, which is made of a number of genes. The objective function (or called fitness function) is calculated for each chromosome based on its genes using the objective function (process model). Populations will be repeatedly modified by some operators (crossover-mutation) to reach the solution which would be the best chromosome. At each generation, the GA selects the chromosomes from the current population based on their scores to represent the parents and uses them to produce offsprings for the next generation. Over successive generations, the population evolves toward an optimal solution [17].

2. Experimental

2.1. Catalyst preparation

Ethylene glycol (EG), citric acid monohydrate, $Zn(NO_3)_2.6H_2O$ and $Cr(NO_3)_3.9H_2O$ were obtained from Merck company. ZSM-5 was obtained from ZeoChem, Swiss. Zinc chromite catalysts were prepared using three conventional methods for production of nano metal oxides, namely sol gel combustion, co-precipitation and pechini type sol gel [18]. Stoichiometric amounts of Zn $(NO_3)_2.6H_2O$ and $Cr(NO_3)_3.9H_2O$ (Merck) with mole ratio of 1:2 were dissolved together in a minimum amount of distilled water. In the co-precipitation method, aqueous ammonia was subsequently added dropwise into the solutions under continuous stirring at 70 °C to obtain the powder suspension. The suspension was kept at the same temperature for 24 h, filtered, and then washed with deionized water. The solids were dried at 80 °C and finally calcined in air at 700 °C for 6 h. In the sol gel combustion method, an aqueous solution of citric acid was mixed with the metal nitrates solution. The molar ratio of citrate to nitrates was 0.4. The heating was kept to remove extra water in order to form the gel. The temperature was then increased to 200 °C and finally the decomposed gel self-ignited and turned to powdered product. The combusted powder was then calcined at 700 °C for 6 h. In pechini method, citric acid and ethylene glycol were used as the monomers for the formation of the polymeric matrix. Proper amounts of citric acid and ethylene glycol (molar ratio = 1:4) were added to a mixture of stock solutions of metal nitrates. Three major reactions: chelation, esterification, and polymerization successively occurred and black polymeric precursor was formed. Details of the synthetic procedure were described elsewhere [20]. The polymeric gels were calcined in air at 200 °C for 6 h, and then heat-treated in air at 700 °C for 6 h.

The supported catalysts were prepared by pechini method with the ratio of spinel to support 2:1.

2.2. Catalyst characterization

X-ray diffraction (XRD) measurements were carried out on a SIEMENS D5000 X-ray powder diffractometer equipped with a Kristalloflex 760 X-ray generator provided with curved graphite monochromator and Cu K_α radiation source (40 kV and 30 mA). The integration time was 3 s per step. Infrared (IR) spectra were recorded with a Bruker 27 FT-IR spectrometer using the Universal ATR Accessory in the range from 3650 to 400 cm^{-1} with 4 cm^{-1} resolution. SEM characterization was carried out with a scanning electron microscope (model EQ-C1-1).

Measurement of the reducibility of different oxides (TPR) was carried out with Micromeritics Autochem 2910 analyzer. Catalyst samples were pre-treated in air at 500 °C for 1 h in order to clean the catalyst surface before reduction. Hydrogen consumption was measured with a flow of a mixture of 10 vol % H_2 in argon with flow rate 50 cm^3/min and a linear heating rate of 10 °C/min, 50–900 °C.

In situ X-ray diffraction (XRD) patterns during the reduction of Zn–Cr mixed oxides were obtained on a PANalytical X-ray diffractometer using Ni-filtered Cu Kα radiation (λ = 1,5406 Å, 45 kV, 40 mA). Catalyst samples were pre-treated in air at 500 °C for 1 h in order to clean the catalyst surface before reduction. XRD profiles, under flowing H_2/Ar gas (mol%, 50 mL(N)/min), were measured at different temperatures (room temperature, 373, 473, 573, 673, 773, 873, 973, 1023 and 1073 K) by scanning steps (step size, 0.033°) in the 2θ ranges between 4° and 90°, with a ramp of 5 K/min. Analyses were performed in a chamber (Anton Paar XRK900) that allows increasing temperature under different flowing gases.

The BET surface area and pore volume of the prepared catalysts were determined by means of N_2 isotherms measured at –196 °C by using a micro pore analyzer (ASAP 2010, USA).

2.3. Evaluation of catalytic performance

The catalysts were tested in toluene combustion at atmospheric pressure and different temperatures in a fixed-bed reactor placed in a PID controlled electrical furnace.

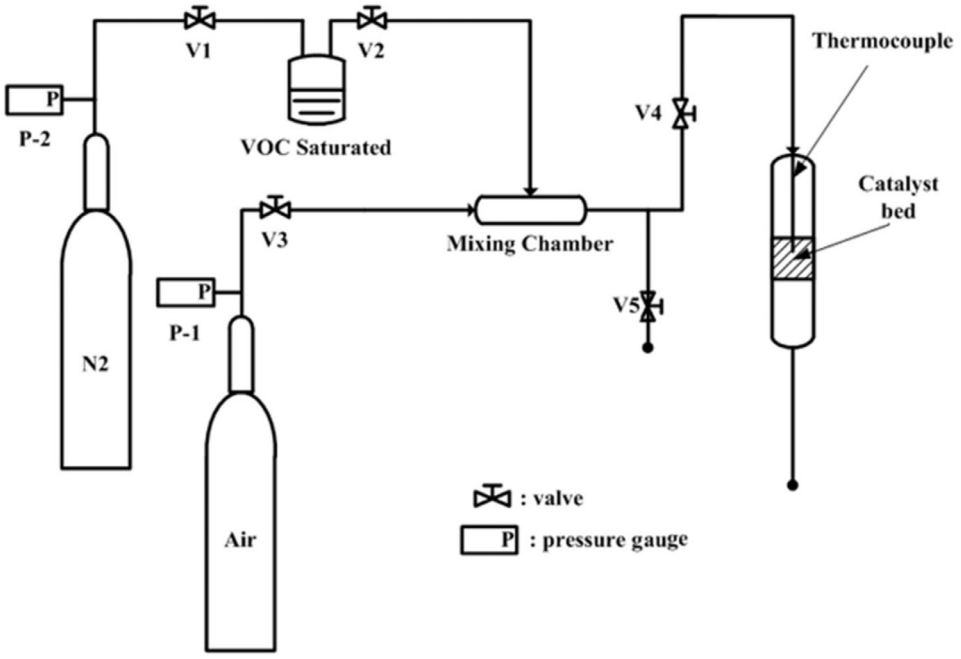

Fig. 1. Schematic diagram of reaction setup for catalytic oxidation of VOCs.

Fig. 1 shows the schematic view of the setup used for catalytic study of VOCs combustion. For each test, 200 mg of catalyst was loaded into a tubular glass reactor with a length of 40 cm and internal diameter of 8 mm. The temperature was controlled with a thermocouple placed inside the catalyst bed. Before starting each run, catalysts were pre-treated with 10 ml/min of pure nitrogen at 400 °C in order to eliminate the possible compounds adsorbed on the catalyst surface. After this pretreatment, the reactor was cooled to 100 °C, and the reaction vapor was introduced by passing the carrier gas (nitrogen) flow through a saturator containing the liquid organic compound (toluene). Flow rates were measured using a soap bubble flow meter. The determination of inlet and outlet concentrations of toluene was carried out in a Shimadzu 2010 gas chromatograph. All experimental runs were taken under steady state conditions.

2.4. Experimental design and method of analysis

Pechini synthesis method, which gave in this work, the most active catalyst, is based on hydrolysis and condensation reactions, and their relative rates are function of many parameters, such as pH, temperature, nature and concentration of the metal ion precursors and concentration of water. Above reactions continue to occur until the solid is dried. After that, only condensation and solid state reactions occur. Thus, aging, drying, and calcination conditions also affect the extent of branching and cross-linking, as well the properties of the final oxide [21].

The first step of the multivariate studies was carried out aiming to screen the effect of different factors in pechini synthesis method. According to literature, three main factors, which play a role during the synthesis process, were selected: calcination temperature, amount of fuel/complexing agent (citric acid), and the ratio of citric acid/ethylene glycol.

The amount of citric acid during the synthetic process is relevant since the formation of citric complexes balance the difference in individual behavior of ions in solution, resulting in a better distribution of ions. Ethylene glycol produces esterification of metallic citrates, resulting in the gelation of reaction mixture. Its addition adjusts the viscosity of the solution and controls the moving velocity of the metal ions. Citric acid/EG ratio influences the extent of branching and cross-linking. Further heating of this precursor results in the formation of the required material with a high degree of homogeneity and dispersion [22,23].

Calcination represents a critical stage in the synthesis, since important processes occur: loss of the chemically bonded water or CO_2, modification of the texture through sintering, modification of the structure, active phase generation and stabilization of mechanical properties [24].

Herein, the design and optimization study of the synthesis factors of $ZnCr_2O_4$ by pechini method was carried out by means of Box–Behnken design under response surface methodology (RSM). Three synthesis factors including calcination temperature, amount of complexing/fuel agent (citric acid), and the ratio of citric acid/ethylene glycol were considered and shown with X_1, X_2, and X_3, respectively. All experiments for modeling were run based on the experimental design matrix (Table 1).

Different linear and quadratic models with different terms were evaluated to fit the experimental data. Finally, a quadratic polynomial equation was selected to predict the response as a function

Table 1
Experimental design matrix, variable levels.

X_1	X_2	X_3	Response
0	0	0	61
−1	1	0	76
1	−1	0	64
0	−1	1	77
0	0	0	59
−1	0	−1	93
−1	0	1	78
0	0	0	60
0	1	−1	71
0	1	1	58
1	1	0	56
1	0	−1	66
1	0	1	63
−1	−1	0	95
0	−1	−1	90

Table 2
GA setting options for optimization.

GA option	Value/function name
Generation size	1000
Population size	50
EliteCount	4
Crossover fraction	0.9
Crossover function	Two point
Selection function	Tournament
Hybrid function	Fmincon
Mutation function	adaptfeasible

of independent factors and their interactions [25]. In general, the response for the quadratic polynomials is described in Eq. (1).

$$Y = \beta_0 + \sum_{j=1}^{3} \beta_j X_j + \sum_{j=1}^{3} \beta_{jj} X_j^2 + \sum_{i<j} \beta_{ij} X_i X_j \quad (1)$$

where Y indicates the predicted response (toluene conversion), β_0 is the intercept coefficient, β_j are the linear terms, β_{jj} are the squared terms, β_{ij} are the interaction terms and X_i and X_j represent the uncoded of independent factors.

The coefficients of the models for the three responses were estimated with multiple regression analysis. The fit quality of the models was judged over their coefficients of correlation and determination. The adequacy of each model was checked with the analysis of variance (ANOVA) [25,26]. The significance of the equation parameters for each response was assessed by p-value andStudent's t-test. The significance test of regression is attemptedto determine the relationship between the response factor and a subset of the independent factors. The prediction of optimum experiment was carried out using genetic algorithm.

2.5. Optimization routine

In this work, the GA methodology was applied to find the optimum conditions of catalyst that maximize toluene conversion. The genetic algorithm (GA) contained in MATLAB optimization Toolbox was used for optimization. In our GA optimization procedure, each chromosome consisted of three genes with various number of bits based on utilized precision for variables (calcinations temperature, molar ratio of citrate to nitrate, molar ratio of citrate to ethylene glycol). Table 2 shows the all setting used for optimization.

3. Results and discussion

3.1. Characterization results

X-ray diffraction patterns of zinc chromite samples resulted from different synthesis methods were taken to determine the crystalline phases of the samples (Fig. 2). The characteristic peaks of zinc chromite spinel, $ZnCr_2O_4$ (JCPDS 22-1107) are observed for all the samples, although the intensity of diffraction lines differ among the different diffractograms.

The characteristic peaks of $ZnCr_2O_4$ (Pech) are sharp and it means that the mean crystallite size of $ZnCr_2O_4$ (Pech) are larger than that of others. In addition, from the sharpest peak ($2\Theta = 35.6$) the mean crystallite size of $ZnCr_2O_4$ in the samples was estimated by the Scherrer equation, being found 23, 33, and 22 nm for the samples obtained by sol gel, pechini, and co-precipitation, respectively.

The formation of spinel structure in the samples was confirmed by FTIR spectroscopy (Fig. 3).

The appearance of two bands in 700–400 cm^{-1} reveals the vibration of metal-oxygen bonds in the spinel structure. Herein, the band around 500 cm^{-1} is attributed to the vibration of Zn–O in the tetrahedral environment and the band above 600 cm^{-1} corresponds to the vibration of chromite in the octahedral (Oh) site of spinel [27,28].

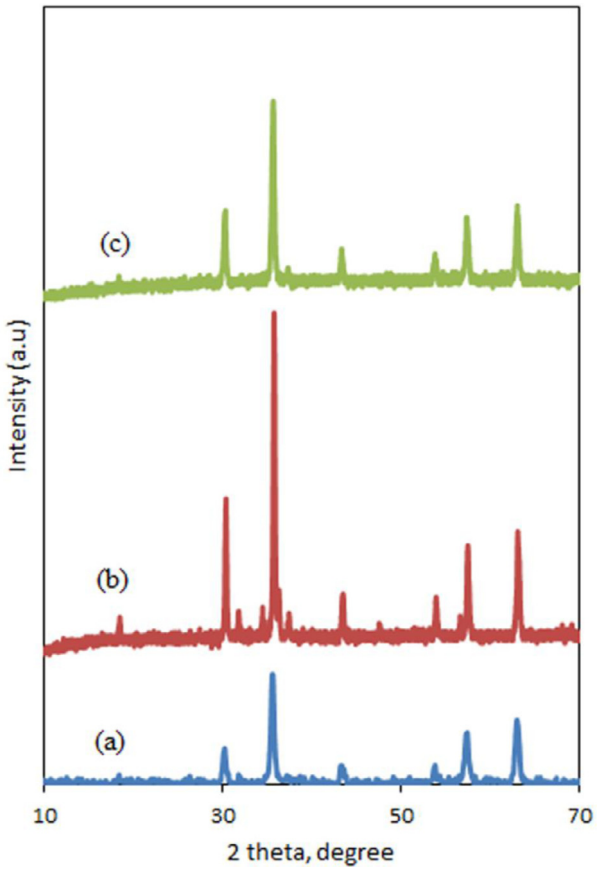

Fig. 2. XRD patterns of oxides, (a) $ZnCr_2O_4$ (sol gel), (b) $ZnCr_2O_4$ (pechini), (c) $ZnCr_2O_4$ (co-precipitation).

The morphology and particle size of $ZnCr_2O_4$ samples are compared by scanning electron microscopy. The SEM images of samples are shown in Fig. 4. The morphology of all samples looks similar and comprised from spherical grains, but the grains of $ZnCr_2O_4$(pechini) and $ZnCr_2O_4$(sol gel) look more uniform and smaller than the particles of $ZnCr_2O_4$ (CP), which are more agglomerated and present larger particle sizes compared to the others.

The reducibility of supported (ZnCr/ZSM-5 (2:1) and ZnCr/γ-Al_2O_3 (2:1)) and unsupported ZnCr samples obtained from different methods was studied by temperature programmed reduction and obtained profiles are shown in Fig. 5.

Two prominent peaks are shown in the profile corresponding to sample ZnCr (Pech). The sharp peak centered around 450 °C is assigned to the reduction of Cr^{6+} existing in another surface phase such as $ZnCrO_4$ [29–31]. The peak around 635 °C is attributed to the reduction of ZnO particles on the surface of the spinel, not incorporated to the spinel lattice during the synthesis [32,33]. The shoulder observed around 300 °C is assigned to the reduction of CrO_3 particles. This contribution attributed to the reduction of chromia phase is more evident in the reduction profile of samples prepared by sol–gel method. It is also observed, in the profile of sample prepared by sol–gel, a hydrogen consumption contribution around 500 °C, ascribed to the reduction of $ZnCrO_4$ phase. As indicated for sample prepared by pechini method, that contribution placed above 600 °C could correspond to the reduction of ZnO particles. For this sample, in comparison to that prepared by pechini

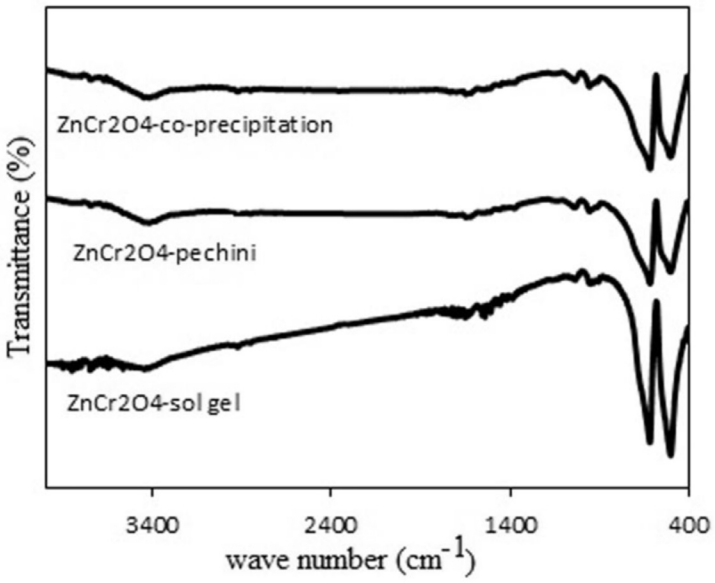

Fig. 3. FTIR spectra of zinc chromite samples.

method, it seems that the reduction peak of this phase is shifted to some higher temperature. Since $ZnCr_2O_4$ is thermodynamically very stable, no reduction peaks of this phase are expected.

For the sample prepared by co-precipitation, the hydrogen consumption around 250–350 °C is ascribed to the reduction of chromia phase. The second contribution, above 700 °C is attributed to the reduction of ZnO particles.

The reduction profiles of $ZnCr_2O_4$–Al_2O_3 and $ZnCr_2O_4$–ZSM-5 are similar and compared to the reduction profiles of unsupported samples, shifted to lower temperatures. Comparing the profiles of these supported samples, the one corresponding to the mixed oxide supported on alumina is shifted to higher temperatures. This fact is explained by a higher interaction of chromium and/or zinc oxides on alumina surface, influenced by the surface hydroxyls distribution [34]. On the other hand, the possible formation of surface chromium aluminates, as small particles, not observed by XRD, could decrease the surface chromia oxygen mobility [35].

The first reduction peak, with a maximum placed around 285 °C for ZnCr-supported on ZSM-5 and around 360 °C, for the sample supported on alumina, is attributed to the reduction of surface CrO_3 particles. The wide reduction contribution centered around 485 and 565 °C for ZSM-5 and alumina-supported zinc chromite, respectively, is explained by the reduction of Cr^{6+} to Cr^{3+} in $ZnCrO_4$ mixed oxide. Finally, above 650 °C, hydrogen consumption is explained by the reduction of ZnO phase.

The fact that these phases, found in the reduction profiles of all the samples, have not been detected by XRD, indicate that their crystalline domain should be lower than 2–3 nm and, therefore, undetectable by X-ray diffraction.

As observed by XRD, the sample $ZnCr_2O_4$ (sol–gel) was the only one, among all the prepared samples, that contained another crystalline phase different from Zn–Cr mixed oxide in a particle size large enough to be detected by this technique. Thus, in this sample, all the diffraction lines corresponds to $ZnCr_2O_4$ (JCPDS 00-022-1107) with the exception of those placed at 31.8, 34.5, 36.3 and 56.6°, which correspond to a minor amount of ZnO (JCPDS 01-075-0576). In order, to confirm the interpretation of TPR results, structural evolution during reduction was studied by in-situ XRD and the diffraction patterns obtained during the reduction is shown in Fig. 6, illustrate the temperature at which ZnO reduction occurs. It can be observed that the reduction of ZnO starts around or below 700 °C and it is completed at 750 °C, which is in accordance with TPR discussion. Metallic Zn is not observed, most likely because the particle size is too small to be detected by this technique.

3.2. Catalyst performance

The catalytic activity of samples was tested in catalytic combustion of toluene. Activity of the catalysts is expressed as conversion of toluene as a function of the reaction temperature in range 150–350 °C. The results of activity tests (toluene conversion) found for the three unsupported catalysts (depicted in Fig. 7) show a good catalytic performance of $ZnCr_2O_4$ in all the cases. Some differences are found between 100 and 200 °C, but at higher temperature the performance of catalysts is approximately the same. Thus, complete conversion of toluene over $ZnCr_2O_4$ resulted at 250 °C. To compare the catalytic performances of the samples, lower reaction temperatures were considered. $T_{80\%}$, temperature for which 80% of toluene is converted, is 100, 127, and 150 °C on ZnCr (Pech), ZnCr (SGC), and ZnCr (CP) samples, respectively. Considering the conversion of toluene at range 100–200 °C, it resulted that the $ZnCr_2O_4$ (Pech) is more active than other unsupported catalysts. The results of this work, in agreement with other research results, pointed out that synthesis method has a prominent effect on activity and physical chemical properties of catalysts [36,37].

Furthermore, the activity of supported catalysts, *i.e.* $ZnCr_2O_4$–ZSM-5 and $ZnCr_2O_4$–Al_2O_3, was evaluated in the catalytic oxidation of toluene. In order to compare the activity of catalysts, the rate of toluene conversion per gram of ZnCr-oxide over catalysts was calculated where were 2.8×10^{-5}, 7.66×10^{-5}, and 4.3×10^{-5} mol/min.g_{cat} over $ZnCr_2O_4$, $ZnCr_2O_4$–ZSM-5 and $ZnCr_2O_4$–Al_2O_3, respectively.

The results show that the rate of toluene conversion over supported catalysts is much higher than that on unsupported catalysts. It is observed that the supporting decreases the reduction temperature of mixed oxides (Fig. 5). It should be noted that the activity and reducibility of the catalysts for this oxidation reaction follow an opposite trend. According to the TPR, higher activity of $ZnCr_2O_4$–ZSM-5 compared to $ZnCr_2O_4$–Al_2O_3 was expected. On the other hand, by considering the specific surface area of $ZnCr_2O_4$–ZSM-5 (85.7 m^2/g) and $ZnCr_2O_4$–Al_2O_3 (62.4 m^2/g) it resulted in a relationship between activity and surface area of the catalysts.

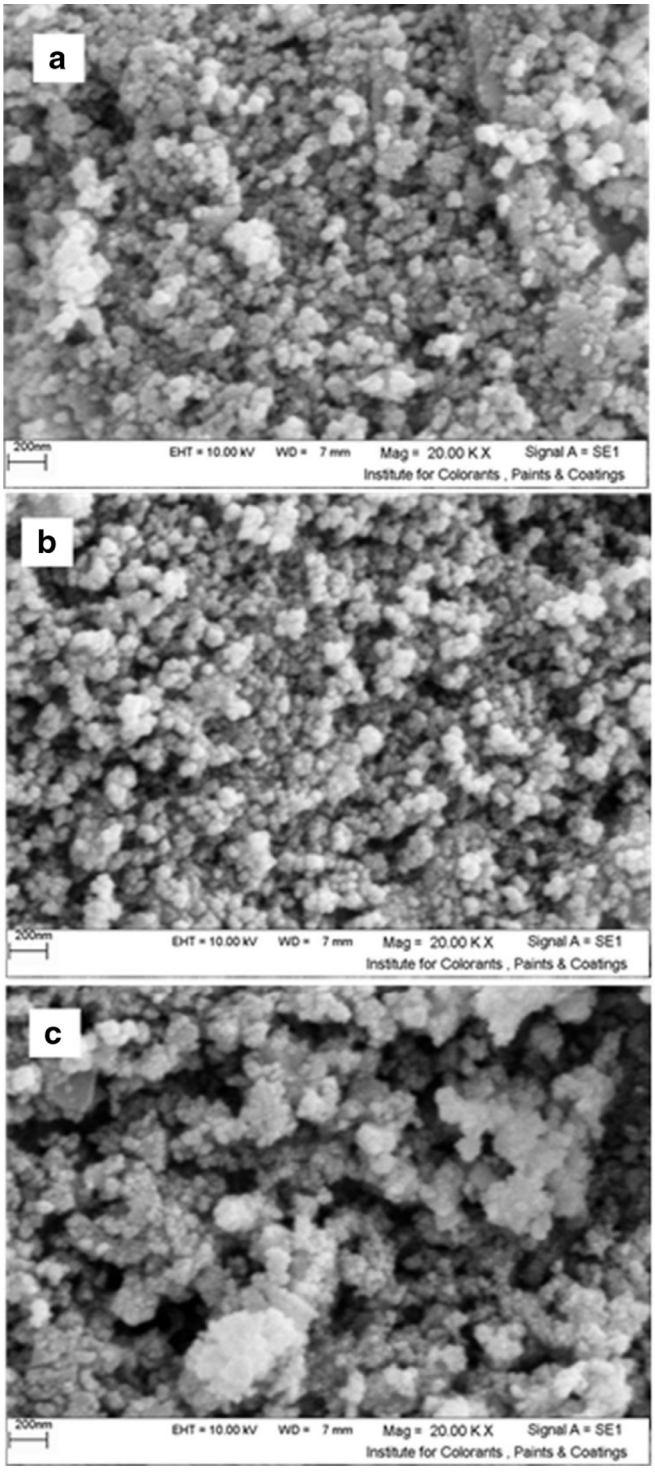

Fig. 4. SEM images of zinc chromium oxides, a (sol gel), b (pechini), c (co-precipitation).

3.3. Results of RSM modeling

Response surface methodology (RSM) was applied to design of experiment and to model the synthesis conditions of $ZnCr_2O_4$ by pechini method. Design of experiment and modeling of synthesis condition were carried out by Box–Behnken method. Among different evaluated models, a model which could best fit the experimental results is presented below.

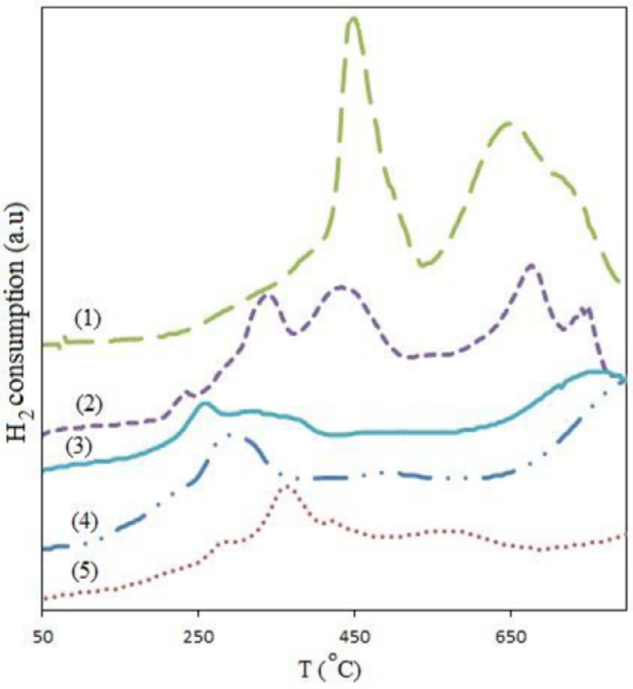

Fig. 5. TPR profiles of chromite catalysts: (1) $ZnCr_2O_4$ (pechini); (2) $ZnCr_2O_4$ (sol gel combustion); (3) $ZnCr_2O_4$ (co-precipitation); (4) $ZnCr_2O_4$/ZSM-5; (5) $ZnCr_2O_4/\gamma$-Al_2O_3.

Table 3
Multiple regression results and sorted significance effect of regression coefficient for toluene conversion.

Term	Coef	SE Coef	T	P
Constant	60.00	1.3994	42.875	0.000
X_1	−11.625	0.8570	−13.565	0.000
X_2	−8.125	0.8570	−9.481	0.000
X_3	−5.500	0.8570	−6.418	0.001
$X_1 * X_1$	6.875	1.2614	5.450	0.002
$X_2 * X_2$	5.875	1.2614	4.658	0.003
$X_3 * X_3$	8.125	1.2614	6.441	0.001
$X_1 * X_2$	2.750	1.2119	2.269	0.046
$X_1 * X_3$	3.000	1.2119	2.475	0.048

$S = 2.42384$ PRESS = 397.75
R-sq = 98.55% R-sq(pred) = 83.62% R-sq(adj) = 96.61%.

$$Y = 60 - 11.625X_1 - 8.12X_2 - 5.5X_3 + 6.87X_1X_2 + 5.87X_2^2 + 8.12X_3^2 + 2.75X_1X_2 + 3.00X_1X_3 \quad (2)$$

Table 3 shows the results of the quadratic response surface model fitting in the form of analysis of variance (ANOVA).

The appropriateness of the models is judged by the determination coefficient (R^2), which reveals a total variation of the observed values of the activity about the average [38]. In foregoing model, the regression coefficients are estimated with a satisfactory determination coefficient of 0.9855 (Fig. 8). The R^2 value means an acceptable agreement between the experimental and predicted values of the fitted model.

Analysis of variance (ANOVA) by F-test was applied to investigate the suitability of the model. In general, the calculated F-value should be several times greater than the tabulated value for the model to be considered as desired one. In fact, the calculated F-value corresponding to 2-propanol conversion is 50.90 and exceeds from tabulated F-value ($F = 8$).

The coefficients are sorted according to their significance to toluene conversion model as indicated by both t- and p-values. The p- and t-values are used to check the significance of each term at

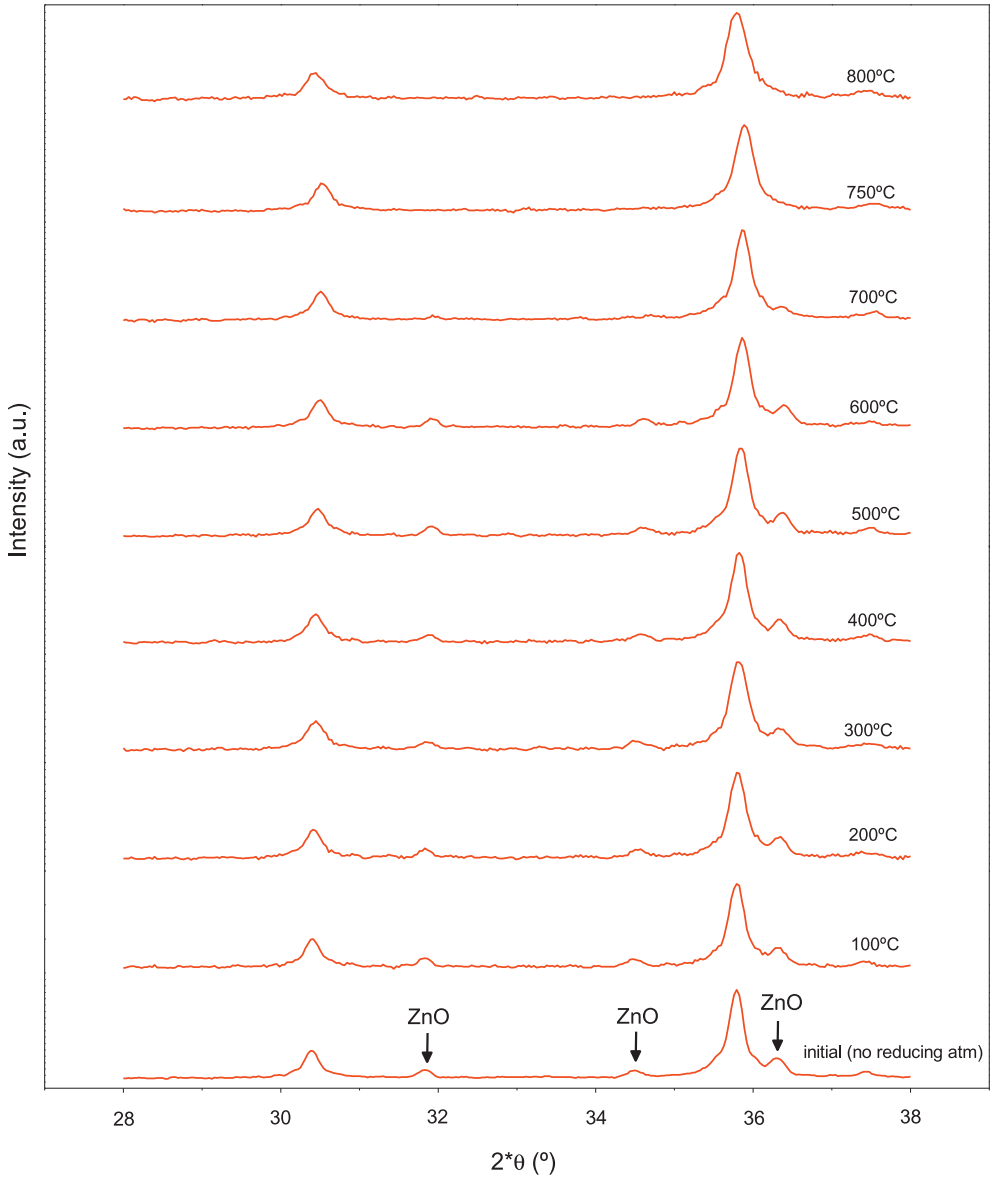

Fig. 6. In-situ XRD patterns obtained under reducing flow (H_2-Ar, 10% mol H_2) for sample $ZnCr_2O_4$ sol–gel.

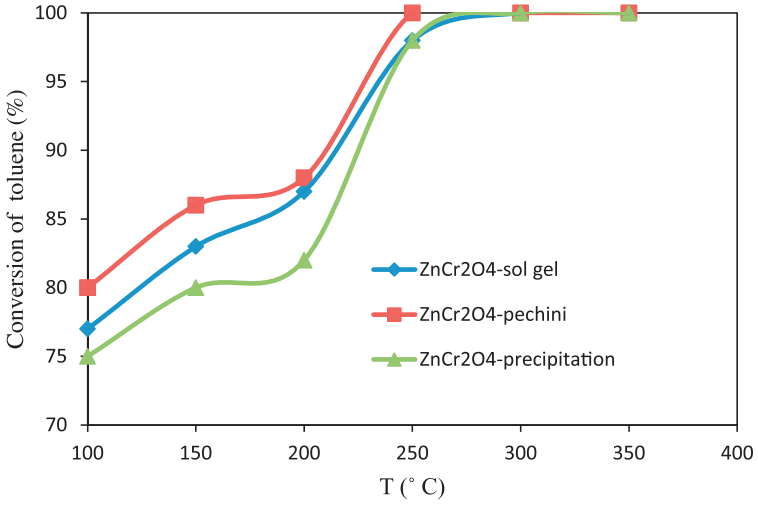

Fig. 7. Catalytic combustion of toluene over $ZnCr_2O_4$-obtained from different methods.

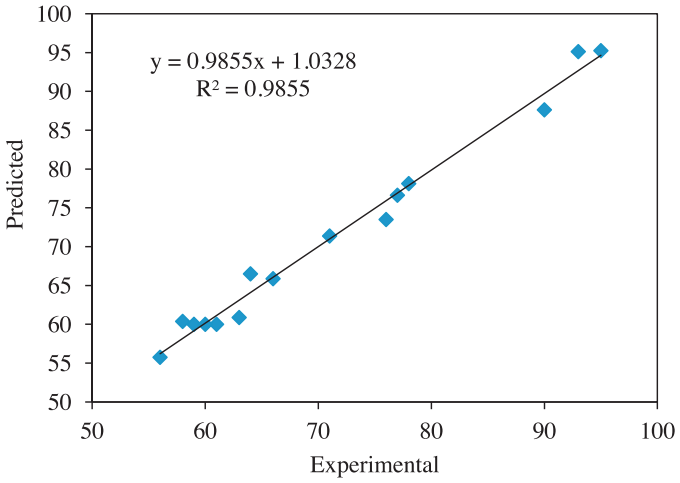

Fig. 8. Correlation curve of experimental response *versus* predicted response.

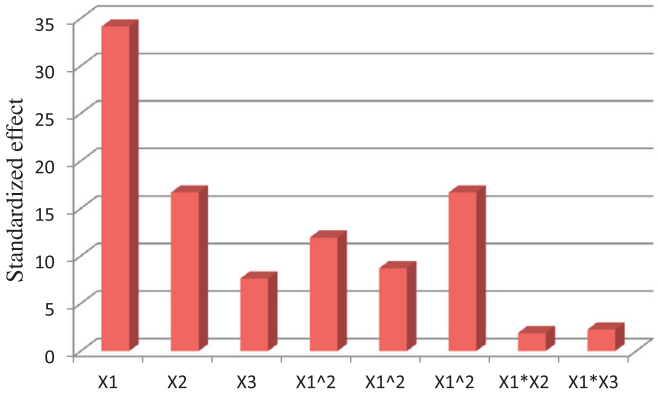

Fig. 9. Pareto analysis.

a specified level of significance [25]. In the table, the one-factor terms represent a linear effect of the corresponding factor, while the two-factor terms represent the interaction between two factors. Through consideration of coefficient of main factors, it is revealed that the calcination temperature had the most prominent effect on the response. In the model, the effect of x_1 (calcination temperature) and x_2 (ratio of [citrate/nitrate] on response were at 100% confidence level, whereas x_3 (ratio of [citrate/EG]) was at 99% confidence level (Table 3). x_1, x_2 and x_3 show antagonistic effect with response.

In addition, the second-order terms represent a quadratic effect toward the response. The smaller p-value means that the corresponding coefficient is more significant.

The terms of x_1x_2 and x_1x_3 indicate the interaction between calcinations temperature with [citrate/nitrate] and [citrate/EG] ratios, respectively.

Among quadratic terms in the model, x_1x_2 with the highest coefficient value (2.75) and t-value (2.269) showed larger effect on conversion of toluene at 96% confidence level of significance, as indicated by the lowest p-value (< 0.046).

The relative importance of each term of the model on the response was predicted by Pareto analysis (Fig. 9). The result of the Pareto analysis revealed that the order of relative importance of independent factors on response is as follows: $x_1 > x_2 > x_3$. This means that the calcination temperature is the factor which affects the most the activity of $ZnCr_2O_4$ nanospinel.

Fig. 10a presents the contour plots of toluene conversion calcination temperature (x_1) and [citrate/nitrate] (x_2). It is observed that the conversion increased with a decrease in both factors in the catalysts and calcination temperature. In agreement with the results of Table 3, the figure reveals that the response increases with the decrease of calcination temperature and mole ratio of citric acid/ethylene glycol in the catalyst. The results are in agreement with those reported in literature. It was found that the increase of calcination temperature decreases the catalytic

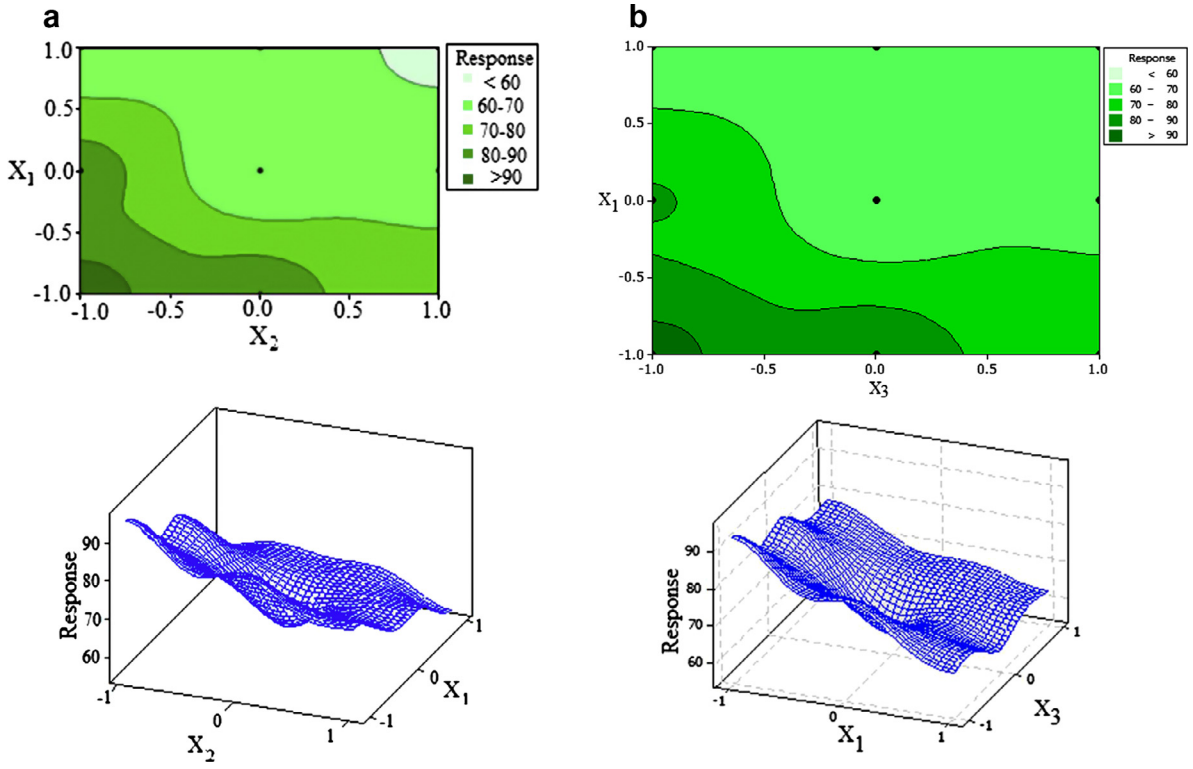

Fig. 10. Contour plots of variable interaction.

activity [38]. Fig. 10b presents the contour plot of x_1 (calcination temperature) and ratio of [citrate/EG]. As it is observed, high response is found at lower value of both x_1 and x_3.

3.4. Optimization using genetic algorithm

The optimal condition for synthesis of $ZnCr_2O_4$ by pechini method was predicted by genetic algorithm. The optimum condition is found at level of –1, –1, and 0 for calcination temperature, [citrate/nitrate], and [citrate/ethylene glycol], respectively. Moreover, there is a good agreement between model prediction and experimental data for optimum catalysts. Thus, under optimal conditions, the conversion of toluene was 97 and 95%, respectively.

4. Conclusions

$ZnCr_2O_4$ nanospinels were successfully synthesized by three conventional methods (pechini, sol-gel and co-precipitation) and tested in the catalytic combustion of toluene. The sample obtained by pechini method exhibited the highest activity. The correlation of physicochemical properties and catalytic activities was investigated.

The pechini method was selected as best method and $ZnCr_2O_4$/ZSM-5 and $ZnCr_2O_4/\gamma$-Al_2O_3 were synthesized by this method.

Supporting of the spinel improved the activity of the catalyst, being found $ZnCr_2O_4$/ZSM-5 more active than $ZnCr_2O_4/\gamma$-Al_2O_3, which is explained by the greater reducibility of supported $ZnCr_2O_4$ and highest surface area compared to unsupported one.

The modeling and optimization of synthesis factors of pechini were successfully carried out by response surface methodology and genetic algorithm, respectively. The model predicted that the calcination temperature of the catalyst was predicted as the most important factor among considered factors.

Acknowledgments

The authors are thankful to Iranian Nanotechnology Initiative Council for financial supports. Especially thanks Prof. Niaei for his assistance in catalytic process.

References

[1] Vu VH, Belkouch J, Ould-Dris A, Taouk B. Catalytic oxidation of volatile organic compounds on manganese and copper oxides supported on titania. AIChE 2008;54:1585–91.
[2] Hosseini SA, Salari D, Niaei A, Deganello F, Pantaleo G, Hojati P. Chemical-physical properties of spinel $CoMn_2O_4$ nano powders and catalytic activity in the 2-propanol and toluene combustion: effect of the preparation method. J Environ Sci Health A 2011;46:291–7.
[3] Wu JCS, Chang TY. VOC deep oxidation over Pt catalysts using hydrophobic supports. Catal Today 1998;44:111–18.
[4] Li WB, Wang JX, Gong H. Catalytic combustion of VOCs on non-noble metal catalysts. Catal Today 2009;148:81–7.
[5] Niaei A, Salari D, Hosseini SA. Study of catalytic activities of nanostructure copper and cobalt supported ZSM-5 catalysts for conversion of volatile organic compounds. Turk J Chem 2010;34:15–25.
[6] Fan Y, Lu X, Ni Y, Zhang H, Zhao L, Chen J. Destruction of polychlorinated aromatic compounds by spinel-type complex oxides. Environ Sci Technol 2010;44:3079–84.
[7] Mehandjiev D, Naydenov A, Ivanov G. Ozone decomposition, benzene and CO oxidation over $NiMnO_3$-ilmenite and $NiMn_2O_4$-spinel catalysts. Appl Catal A 2001;206:13–18.
[8] Shangguan WF, Teraoka Y, Kagawa S. Simultaneous catalyticremoval of NOx and diesel soot particulates over ternary AB_2O_4 spinel-type oxides. Appl Catal B. 1996;8:217–27.
[9] Bhattacharyya AA, Woltermann GM, Yoo JS, Karch JA, Cormier WE. Catalytic SOx abatement-the role of magnesium aluminate spinel in the removal of SOx from fluid catalytic cracking (FCC) flue-gas. Ind Eng Chem Res 1988;27:1356–60.
[10] Jebarathinam NJ, Eswaramoorthy M, Krishnasamy V. Non oxidative and oxidative dehydrogenation of ethyl benzene over Zn-Fe-Cr ternary spinel system. Appl Catal, A 1996;145:57–74.
[11] Kim DC, Ihm SK. Application of spinel-type cobalt chromite as a novel catalyst for combustion of chlorinated organic pollutants. Environ Sci Technol 2001;35:222–6.
[12] Zavyalova U, Nigrovski B, Pollok K, Langenhorst F, Müller B, Scholz P, et al. Gel-combustion synthesis of nanocrystalline spinel catalysts for VOCs elimination. Appl Catal B. 2008;83:221–8.
[13] Qian M, Zeng HC. Synthesis and characterization of Mg–Co catalytic oxide materials forlow-temperature N_2O decomposition. J Mater Chem 1997;7:493–9.
[14] Markov L, Lyubchova A. Precursor control of the inversion degree of magnesium-cobalt spinels. J Mater Sci Lett 1991;10:512–14.
[15] Hosseini SA, Niaei A, Salari D, Nabavi SR. Nanocrystalline AMn_2O_4 (A = Co, Ni, Cu) spinels for remediation of volatile organic compounds—synthesis, characterization and catalytic performance. Ceram Int 2012;38:1655–61.
[16] Hosseini SA, Alvarez-Galvan MC, Fierro JLG, Niaei A, Salari D. MCr2O4 (M = Co, Cu, Zn) nano spinels for 2-propanol combustion: correlation of structural properties with catalytic performance and stability. J Ceram Int 2013;39:9253–61.
[17] Hosseini SA, Niaei A, Salari D, Alvarez-Galvan MC, Fierro JLG. Synthesis, characterization and catalytic activity of Cu-(Cr, Mn and Co)$_2$ nano mixed oxides in VOC combustion -Study of correlation between activity and structural properties. J Ceram Int 2014;40:6157–63.
[18] Liu W, Farrington GC, Chaput F, Dunn B. Synthesis and electrochemical studies of spinel phase LiMn2 O 4 cathode materials prepared by the pechini process. J Electrochem Soc 1996;143:879–84.
[19] Chong MN, Zhu HY, Jin B. Response surface optimization of photocatalytic process for degradation of Congo Red using H-titanate nanofiber catalyst. Chem Eng J 2012;156:278–85.
[20] Wu S, Su H. Electrochemical characteristics of partially cobalt-substituted $LiMn_{2-y}Co_yO_4$ spinels synthesized by Pechini process. Mater Chem Physic 2002;78:189–95.
[21] Kung HH, Ko EI. Preparation of oxide catalysts and catalyst supports – a review of recent advances. Chem Eng J 1996;64:203–14.
[22] Tai LW, Lessing PA. Modified resin-intermediate processing of perovskite powders. Part I. Optimization of polymeric precursors. J Mater Res 1992;7:502–10.
[23] Kakihana M, Yoshimura M. Synthesis and characterization of complex multicomponent oxides prepared by polymer complex method. Bull Chem Soc Jpn 1999;72:1427–43.
[24] Perego C, Villa P. Catalyst preparation methods. Catal Today 1997;34:281–305.
[25] Clarke GM, Kempson RE. Introduction to the Design and Analysis of Experiments 1997.
[26] Khataee AR, Safarpour M, Naseri A, Zarei M. Photoelectro-Fenton/nanophotocatalysis decolorization of three textile dyes mixture: response surface modeling and multivariate calibration procedure for simultaneous determination. J Electroanal Chem 2012;672:53–62.
[27] Peng C, Gao L. Optical and photocatalytic properties of spinel ZnCrO nanoparticles synthesized by a hydrothermal route. J Am Ceram Soc 2008;91:2388–90.
[28] Grzybowska B, Sloczynski J, Grabowski R, Wcislo K, Kozlowska A, Stoch J, et al. Chromium oxide/alumina catalysts in oxidative dehydrogenation of isobutane. J Catal 1998;178:687–700.
[29] Zwinkels MFM, Haussner O, GovindMenon P, Järås SG. Preparation and characterization of $LaCrO_3$ and Cr_2O_3 methane combustion catalysts supported on $LaAl_{11}O_{18}$- and Al_2O_3-coated monoliths. Catal Today 1999;47:73–82.
[30] Wojciechowska M, Tomska-Foralewska I, Przystajko W, Zieliński M. Catalytic properties of Cr_2O_3 doped with MgO supported on MgF_2 and Al_2O_3. Catal Lett 2005;104:121–8.
[31] Venugopal A, Sarkari R, Anjaneyulu C, Krishna V, Kumar MK. Cu–Zn–Cr_2O_3 catalysts for dimethyl ether synthesis: structure and activity relationship. Catal Lett 2008;123:142–9.
[32] Kam R, Selomulya C, Amal R, Scott J. The influence of La-doping on the activity and stability of Cu/ZnO catalyst for the low-temperature water–gas shift reaction. J Catal 2010;273:73–81.
[33] Gaspar AB, Brito JLF, Dieguez LC. Characterization of chromium species in catalysts for dehydrogenation and polymerization. J Mol Catal A-Chem 2003;203:251–66.
[34] Pradier CM, Rodrigues F, Marcus P, Landaub MV, Kaliya ML, Gutman A, et al. Supported chromia catalysts for oxidation of organic compounds, the state of chromia phase and catalytic performance. Appl Catal B 2000;27:73–85.
[35] Križan J, Možina J, Bajsić I, Matjaž M. Synthesis and fluorescent properties of chromium-doped aluminate nanopowders. Acta Chim Slov 2012;59:163–8.
[36] Abdolrahmani M, Parvari M, Habibpoor M. Effect of copper substitution and preparation methods on the LaMnO structure and catalysis of methane combustion and CO oxidation. Chin J Catal 2010;31:394–403.
[37] Cavani F, Trifiro´ F, Vaccari A. Hydrotalcite-type anionic clays: preparation, properties and applications. Catal Today 1991;11:173–301.
[38] Pecchi G, Campos C, Pena O. Catalytic performance in methane combustion of rare-earth perovskites $RECo_{0.50}Mn_{0.50}O_3$ (RE: La, Er, Y). Catal Today 2011;172:111–17.